AED - R 71 - 10

AEROSPACE ENGINEERING DEPARTMENT

TEXAS A&M UNIVERSITY

SUBSONIC, TRANSONIC, AND SUPERSONIC NOZZLE FLOW BY THE INVERSE TECHNIQUE

1. Nozzle Flow

by

DAVID J. NORTON

TEXAS ENGINEERING EXPERIMENT STATION

SUBSONIC, TRANSONIC, AND SUPERSONIC NOZZLE FLOW BY THE INVERSE TECHNIQUE

BY

DAVID J. NORTON

ASSISTANT PROFESSOR

AEROSPACE ENGINEERING DEPARTMENT

TEXAS A&M UNIVERSITY

JULY 1971

*This work was supported by NASA while the author was stationed at JPL serving as Captain in the United States Army.

ROTATIONAL GAS DYNAMIC FLOW BY THE INVERSE METHOD

Abstract

This paper concerns the use of an inverse method to describe two-dimensional gas dynamic flow fields of either rotational or irrotational character. The inverse method provides a means of solving the elliptic flow equation in the subsonic region, as well as the hyperbolic equation of the supersonic region. This is accomplished by specifying Cauchy conditions such as centerline velocity or pressure as well as their derivatives normal to the centerline. The governing equations are then solved in the half plane by integrating in a direction normal to the streamlines. Each streamline obtained by integrating the governing equations may represent a solid wall contour in the inviscid sense. In this paper the governing equations for inviscid steady, axisymmetric flow are to be solved for several nozzle flow fields. These equations are solved numerically in a transformed system of coordinates representing the stream function and a stretched axial coordinate to permit maximum stability. The unique feature of the method of solution is that it permits a unified treatment of the subsonic (including initial conditions), the transonic and the supersonic portions of a rotational flow.

Background

Two-dimensional calculations for nozzles and wind tunnel have

usually treated the flow in three distinct regimes: the subsonic, the transonic, and the supersonic. While it is true that perturbations in the supersonic flow do not affect the subsonic flow, unless a mach line intersects the sonic line, changes in the subsonic flow do influence the supersonic flow[1]. Since we have a powerful tool for the solution of hyperbolic equations in the Method of Characteristics (MOC), the supersonic flow has received a great deal of attention. Optimum contours can now be calculated which account for a variety of aerothermodynamic effects.

The supersonic flow field solutions by MOC calculations are initiated in the transonic regions from an initial data surface which is a Cauchy boundary condition (the value and their derivatives are known). At first, MOC calculations employed one-dimensional results for this initial data; now, however, special transonic analyses have been derived reflecting in some degree the two-dimensional effects at the throat[2,3,4]. These solutions are characterized by a perturbation analysis about M = 1 for small radial velocities. The nozzle wall at the throat is represented by a finite series of terms not necessarily matching the desired contour. In general, the series of solution is expanded in terms of some function of (R_c/R_t) which causes convergence difficulties for $R_c/R_t < 1$.

An improvement to the above methods was introduced by Kliegel and Levine[5] when, the wall contour is represented by a series suggested by orthogonal torroidal coordinates. This

approach involves an expansion of the wall contour in terms of $1/(R_c/R_t + 1)$. The solution obtained is essentially that of Hall[4] for large R_c/R_t, however, it continues to predict realistic results for $R_c/R_t \approx 1$. Recently Kliegel and Levine have concluded that the series employed does not converge for higher approximations[6].

More recently a special form of the Cauchy nozzle flow problem has been used with great success for calculating the transonic flow in nozzles[7,8]. The basis for this method is to specify a centerline function, and to assume the dependent variables are adequately represented by a finite series involving the independent variables (3 or 4 terms). In this way, a solution for the nozzle wall over a region about the throat is directly obtainable without numerical integration. By proper choice of the centerline Cauchy condition a throat contour and inlet angle may be reasonably matched. It has been possible to calculate the flow field for throat contours of very small radius of curvature ($R_c/R_t < .25$). Unfortunately, this method is difficult to extend far into the subsonic region with a resonable match of the desired wall contour. This is due to the finite number of terms carried in the series representing the dependent variables, and the fact that in the Cauchy approach, points far from the centerline require high order derivatives of the centerline function. Ultimately, of course, all of the above methods do not allow the low subsonic flow field and the method of mass generation (initial conditions)

to influence the transonic and supersonic flow.

The principal reason for the failure of subsonic calculations is the lack of known boundary conditions for a fixed geometry. The classical method of solution of elliptic equations requires boundary conditions of the Newman (derivatives of dependent variables) or Dirichlet (magnitude of the dependent variables) type over a closed region. The solution for the interior points is effected by relaxation allowing the prescribed boundary conditions to determine the interior values. In gas dynamic flows, often these boundary conditions are not known; in fact, these conditions are often the primary purpose of the analysis. This is especially true of the transonic region boundary conditions which are useful for MOC supersonic flow solutions.

It has been argued on the basis of experimental observation that the subsonic flow does not significantly affect the transonic flow. While this may be a justifiable conclusion for the purposes of an initial data surface for MOC calculations, the mathematical consequences of this assumption for subsonic flow are not acceptable. A complete transonic solution provides a Cauchy condition. If this Cauchy condition is employed over any portion of a closed boundary defined by the wall, the centerline, the initial plane, and a reference line in the transonic region the problem is overspecified[9]. To circumvent this problem the initial plane could be left open. We know from experimental results that the method of mass generation at the initial plane does not significantly

influence the transonic region; therefore, it cannot be expected that the transonic solution could be projected back to a unique initial condition unless the transonic solution was extremely accurate.

The only remaining option is to specify the initial conditions and to use only Newman-Dirichlet conditions at the transonic reference line. However, unless the two boundary conditions are exactly correct, the interior flow cannot be expected to relax to a stable value because it is necessary to match the mass energy and momentum exactly.

At the present time there are two methods for eliminating these mathematical difficulties: the inverse Cauchy Method and the Asymptomatic Time Method. The latter makes use of Crocco's suggestion[10] by considering the unsteady flow equations which are hyperbolic with respect to time[11,12]. Under these conditions the Cauchy problem is proper and the solution proceeds from an assumed initial condition for the entire flow fields to a steady state solution, if one exists. This method has recently been shown feasible for flows initiated from an infinite reservoir where the initial velocities are zero. However, for flows originating from a constant area duct, it is necessary to solve the unsteady flow field many times to obtain the proper initial velocity in order to prevent instabilities. The large number of resultant calculations influence the accuracy due to roundoff errors. However, with the advent of faster computers which carry more significant

digits these problems may not be significant.

The inverse Cauchy method can be employed to solve the governing equations efficiently and accurately for an entire flow field without simplifying assumptions[12]. This is accomplished by integrating in steps of the stream function from an analytic, smooth Cauchy centerline condition. The solution obtained is exact; however, the streamlines may not represent the desired shape for a given physical problem. This disadvantage limits the use of this method to a design function unless substantial interation of the centerline function is permitted.

THE INVERSE METHOD

The inverse method allows the solution of nozzle flow problems in the subsonic, transonic and supersonic regions. The method employes an assumed centerline profile. This profile is of the Cauchy type in that the values and the derivatives of the profile are known. For arbitrarily specified centerline data, the solution of the governing flow equations may not exist, and if it does, it may not depend continuously on the data[14]. However, if analytic data is specified, the Cauchy-Kowalewsky theorem[15] indicates that a solution exists in the neighborhood of the initial data. Integration is initiated at the centerline and is continued radially in the half-plane indefinitely, providing instabilities do not develop. In addition to the centerline data, end conditions may be specified, but these may not be of the Cauchy type since these

would over-specify the solution unless they are imposed at $\pm\infty$. However, boundary condition of Dirichlet or Newman type are always permissible. This permits the postulation of rotational types of flow in the sense that entropy may vary normal to the streamlines due to non-uniformities in the combustion or due to tangential velocities.

Recently, there has been some attempts to obtain a mathematically and physically consistent solution of the flow field from mass generation surface through the supersonic region. This is necessary to accurately predict the heat transfer in nozzles with rapidly converging inlets and low radius of curvature throat sections. The rapid convergent section provides a minimum heat path and tends to laminarize the boundary layer thus reducing heat transfer losses[16]. Another important feature in the low subsonic flow field is the flow behavior in the region adjacent to the transition from the constant area combustion chamber and convergent section. It has been found that often boundary layer separation occurs in this concave region due to a locally unfavorable pressure gradient[17].

It is for these types of flow details that the inverse method can be a practical design tool. It is possible to input various centerline velocities profiles and examine nozzle contours with their associated velocity and pressure fields. By logical choice a centerline velocity function can be derived which gives the salient features of a desired nozzle flow field. In this manner,

the flow in the concave region can be studied and a nozzle profile which minimizes the unfavorable pressure gradient in this area can be determined.

From a design point of view, it is possible to input centerline velocity profiles and to obtain a mathematically exact solution to the flow field, such that if a nozzle was constructed with the contour of a streamline thus generated, the exact solution for the flow would be known for the envisioned flow. Furthermore, since the free stream is known, the boundary layer may be calculated so that the wall may be appropriately displaced.

It should be emphasized that the inverse method is not suited to the detailed prediction of an existing nozzle contour. Most nozzles are constructed from simple geometrical shapes such as circular arcs and conical sections which, at their juncture, are discontinuous in the higher order derivatives. Since any centerline velocity must be an analytic function, streamline contours cannot be expected to be discontinuous.

THE ANALYSIS

In this section the governing gas dynamic equations for rotational (non-homentropic), steady flow will be presented. Subsequently, these equations will be transformed into the ψ , ξ plane which represents respectively, the streamline function and a stretched axial coordinate. (See Figure 1)

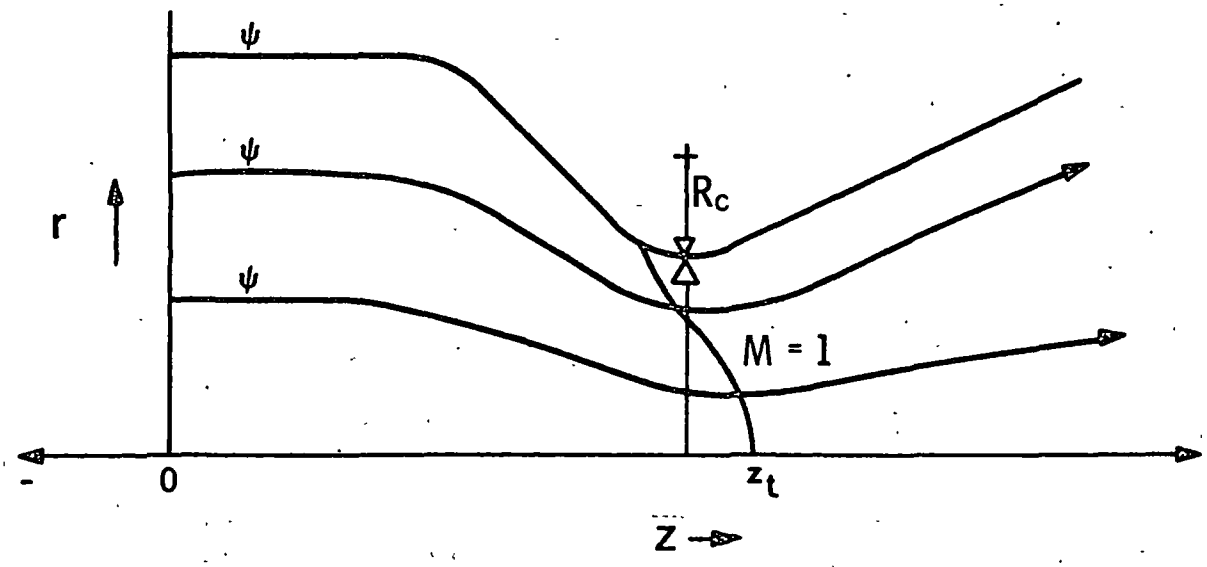

PHYSICAL PLANE NOZZLE CONTOUR

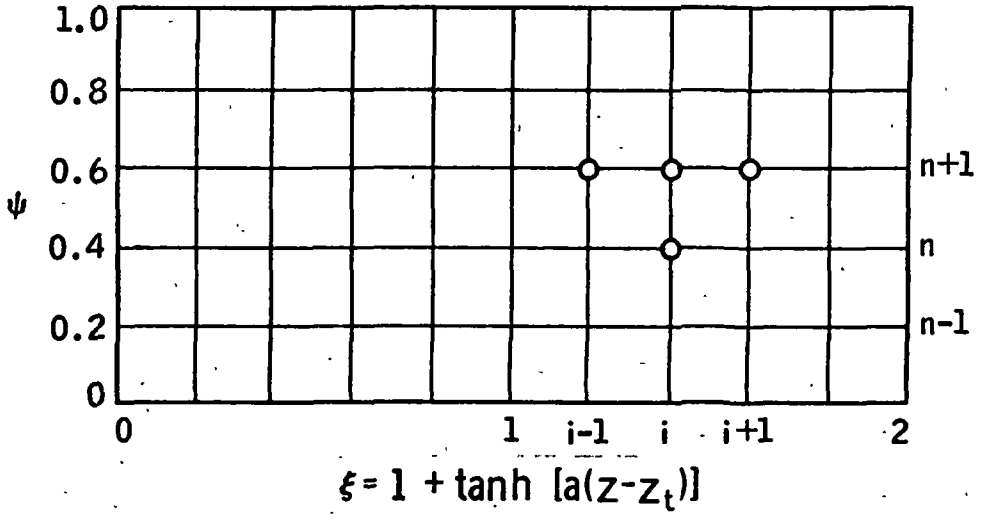

TRANSFORMED PLANE

FIGURE 1. PHYSICAL AND TRANSFORMED COORDINATES

Continuity Equations

$$\frac{\partial \psi}{\partial r} = \rho w r \tag{1}$$

$$\frac{\partial \psi}{\partial z} = -\rho u r \tag{2}$$

Momentum Equations

$$\frac{\partial P}{\partial r} = -\rho\left(u \frac{\partial u}{\partial r} + \frac{w \partial u}{\partial z} - \frac{v^2}{r}\right) \tag{3}$$

$$\frac{\partial P}{\partial z} = -\rho\left(u \frac{\partial w}{\partial r} + \frac{w \partial w}{\partial z}\right) \tag{4}$$

$$\frac{D(vr)}{Dt} = u \frac{\partial (vr)}{\partial r} + w \frac{\partial}{\partial z}(vr) = 0 \tag{5}$$

Process Equation

$$\bar{q} \cdot \nabla S = 0 \tag{6}$$

Energy Equation

$$\bar{q} \cdot \nabla H_o = 0 \tag{7}$$

For the continuity equation a streamline function has been introduced such that continuity is satisfied identically.

$$\frac{\partial^2 \psi}{\partial r \partial z} - \frac{\partial^2 \psi}{\partial r \partial z} = 0 \tag{8}$$

The momentum equations are those of Euler for axisymmetric flow and they are reduced from the Navier-Stokes equations by neglecting the effects of viscosity. The process equation reflects the conservation of entropy along streamlines but it allows variations normal to them. The energy equation is equivalent to the process equation and it assures constant total enthalpy along streamlines.

Transformation of the Governing Equations

Since the equations are to be solved numerically, and it is well known that the Cauchy boundary conditions can give rise to numerical instabilities if not properly handled[18], it was decided to transform the governing equations into a form which puts any geometry into a rectangular shape and which spaces the network of interior points more finely in regions of the greatest gradients of the dependent variables (Figure 1). The transformation is formally stated as:

$$r,z \rightarrow \psi,\xi \tag{9}$$

where

ψ = the stream function of equations 1 and 2.

ξ = the stretched axial coordinate.

The transformation is best handled employing the Jacobian, first noting, however, the functional dependence of ψ and ξ on r and z.

$$\psi = \psi(r,z) \tag{10}$$

$$\xi = \xi(z) \tag{11}$$

The results of the Jacobian yield the paritals of the old independent variables in terms of the new ones.

$$\frac{\partial r}{\partial \psi} = (\rho r w)^{-1} \tag{12}$$

$$\frac{\partial r}{\partial \xi} = (u/w\xi') \tag{13}$$

$$\frac{\partial z}{\partial \psi} = -(\rho r u)^{-1} \tag{14}$$

where,

$$\xi' = \frac{\partial \xi}{\partial z} = \frac{d\xi}{dz} \tag{15}$$

The momentum equation is derived below.

$$\frac{\partial P}{\partial r} = \frac{\partial P}{\partial \psi}\frac{\partial \psi}{\partial r} + \frac{\partial P}{\partial \xi}\frac{\partial \xi}{\partial r} = \frac{\partial P}{\partial \psi}\rho w r \tag{16}$$

$$\frac{\partial P}{\partial r} = \rho w r \frac{\partial P}{\partial \psi} = -\rho\{\frac{u\partial u}{\partial \psi}\rho w r + w[\frac{\partial u}{\partial \xi}\xi'$$

$$- \rho u r \frac{\partial u}{\partial \psi}] \frac{-v^2}{r}\} \tag{17}$$

Collecting terms, and solving for $\partial P/\partial \psi$ yields,

$$\frac{\partial P}{\partial \psi} = \frac{1}{wr}\left[-\frac{w\partial u}{\partial \xi}\xi' + \frac{v^2}{r}\right] \tag{18}$$

The governing equations which apply in the transformed plane are given below where Γ has been introduced as $\Gamma \equiv vr$, which is a function of the circulation and most remain constant along a streamline.

$$\frac{\partial r}{\partial \psi} = 1/\rho rw \tag{19}$$

$$\frac{\partial r}{\partial \xi} = u/w\xi' \tag{20}$$

$$\frac{\partial P}{\partial \psi} = \frac{1}{wr}\left[-\frac{w\partial u}{\partial \xi}\xi' + \frac{\Gamma(\psi)^2}{r^3}\right] \tag{21}$$

$$P = F(\psi)\,\rho^{1/\gamma} = \text{constant on } \psi \tag{22}$$

$$\Gamma = \Gamma(\psi) = \text{constant on } \psi \tag{23}$$

$$H_o(\psi) = c_p T + \frac{u^2 + v^2 + w^2}{2} \tag{24}$$

$$P_o(\psi) = P\left[1 - \frac{\gamma - 1}{2\gamma RT_o(\psi)}\,(u^2 + v^2 + w^2)\right]^{\frac{-\gamma}{\gamma-1}} \tag{25}$$

where $F(\psi)$, $\Gamma(\psi)$, and $H_o(\psi)$ are determined from the specified initial conditions.

The preceding equations are valid for rotational flow with any distribution of tangentials velocity, entropy, and energy

which may be specified as the initial conditions. The boundary conditions for the open boundary are:

$$\xi = 0,\ z = -\infty\ ;\ w(\psi) = f(\psi),\ u(\psi) = 0$$

$$\xi = 2,\ z = +\infty\ ;\ w(\psi) = w_{inf},\ u(\psi) = 0 \qquad (26)$$

$$\psi = 0,\ r = 0\ ;\ w(\xi) = w_{cl},\ u(\xi) = 0$$

The centerline velocity w_{cl} and the stretched axial coordinate are defined only when a particular problem is to be solved.

NOZZLE FLOW

To solve a nozzle flow problem using the inverse technique, it is required that an analytic centerline velocity function be chosen which contains the salient features of the nozzle to be designed. The centerline velocity function must also agree with the end conditions wherever they are applied. A number of functions have been devised by other authors[7,13,18] however, for the present study a function has been developed which has been found to be descriptive of the entire nozzle.

$$\bar{W}_{cl}(z) = M^* = W_{cl}/a^* = 1 + \frac{A}{2}\{\tanh[B(z-z_t)] + \tanh[C(z-z_t)]\} \quad (27)$$

Some of the features of this function are given below:

$$\bar{W}_{cl}(-\infty) = \bar{W}_o = 1 - A \quad (28)$$

$$\bar{W}_{cl}(+\infty) = \bar{W}_{inf} = 1 + A \quad (29)$$

$$\bar{W}_{cl}(z_t) = 1.0 = M^*_t \quad (30)$$

$$\bar{W}'_{cl}(z_t) = \frac{d\bar{W}_{cl}}{dz} = A(B + C)/2 \quad (31)$$

Thus, equation 27 insures that $M^* = 1$ at $z = z_t$, and that the derivative is maximum and independent of z at the throat. Note that z_t does not define the plane of minimum area since the flow properties vary in the radial direction. This function introduces three arbitrary constants which are useful in specifying the contraction ratio, ε_c; the nozzle inlet angle, θ_w; and the radius of curvature ratio, R_c/R_t. The constant A controls ε_c by specifying the velocity at the initial plane. It also controls

the maximum velocity reached in the supersonic portion of the flow. The constants B and C control the radius of curvature ratio for a given ϵ_c by specifying the rate at which velocity changes through the throat. Note that $\bar{W}'_{cl}$ is maximum and independent of z at the throat. From experience it has been found that this criteria forms the streamlines into circular arcs at the throat; thereby permitting comparison with existing experimental work. The nozzle inlet angle, θ_w, is determined by the streamline under consideration and a complicated function of A, B, and C.

Now that the centerline velocity function has been presented it is necessary to discuss the choice of an axial stretching function. Recall that the fundamental postulate of the inverse method is that every point in the flow field depends continuously on the centerline velocity function. In a numerical sense, as ψ is increased more and more of the centerline data is required. If the centerline function can be specified to infinity with boundary conditions along ψ then it is possible to integrate without losing points at either end of the axial coordinate. Also, specifying the centerline function to infinity prevents the propogation of disturbances from arbitrarily imposed boundary conditions, at a finite axial location. Two features appear desirable for the stretching function. First there should be appropriate spacing of points to allow maximum accuracy at all axial locations. This requires the grouping of points at the throat while minimizing the points where the dependent variables are varying little, such as the chamber. Second, the stretching function should facilitate the numerical computation by

putting the physical coordinate z into a finite region.

These objectives were accomplished by specifying a stretched coordinate ξ which was functionally similar to the centerline velocity function. Figure 2 presents the relationship of W_{c_L} and ξ with z.

$$\xi = 1 + \text{Tanh}[a(z-z_t)]$$

$$\xi' = a\ \text{sech}^2[a(z-z_t)] = a\ \xi(2-\xi) \tag{32}$$

$$z = \log(\xi/2 - \xi)/2a + z_t$$

It is readily observed that,

$$\begin{aligned} z &= -\infty ; \quad \xi = 0 \\ z &= z_t ; \quad \xi = 1 \\ z &= +\infty ; \quad \xi = 2 \end{aligned} \tag{33}$$

Initially some useful results were obtained assuming B = C. Figure 3 presents the results for $\gamma = 1.40$, $R_c/R_t = 0.40$, and $\varepsilon_c = 4.0$. To obtain these results, the coefficients of equation (37) were assigned as follows:

$$\begin{aligned} A &= 1 - \frac{1}{\varepsilon_c}\left[\frac{2}{\gamma + 1}\right]^{1/(\gamma - 1)} = .841 \\ B &= C = .975 \\ z_t &= 5.0 \end{aligned} \tag{34}$$

Each streamline can represent a nozzle wall for inviscid flow. Increasing the stream function results in smaller R_c/R_t nozzle

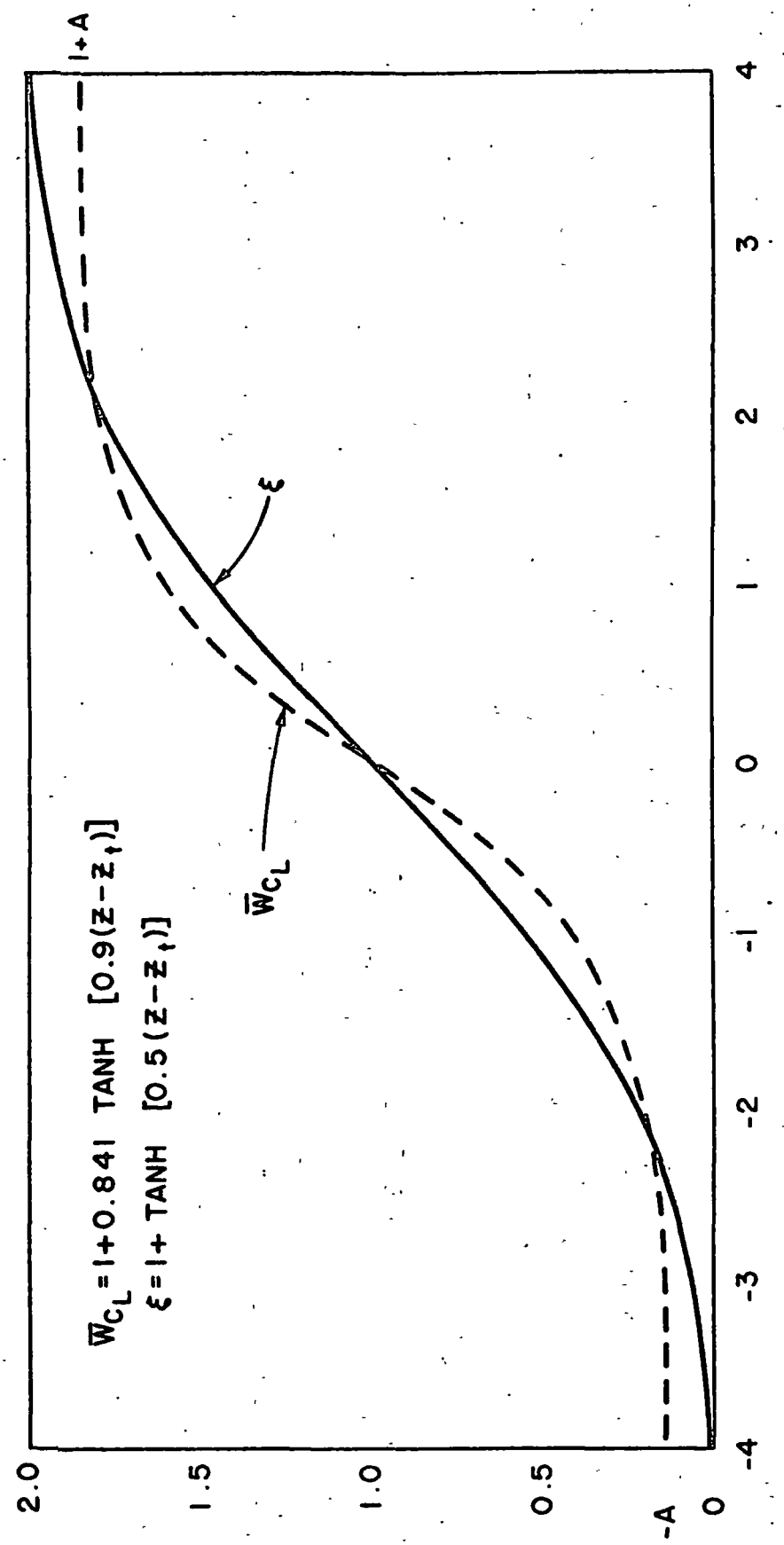

FIGURE 2. TYPICAL CENTERLINE VELOCITY AND AXIAL STRETCHING FUNCTIONS

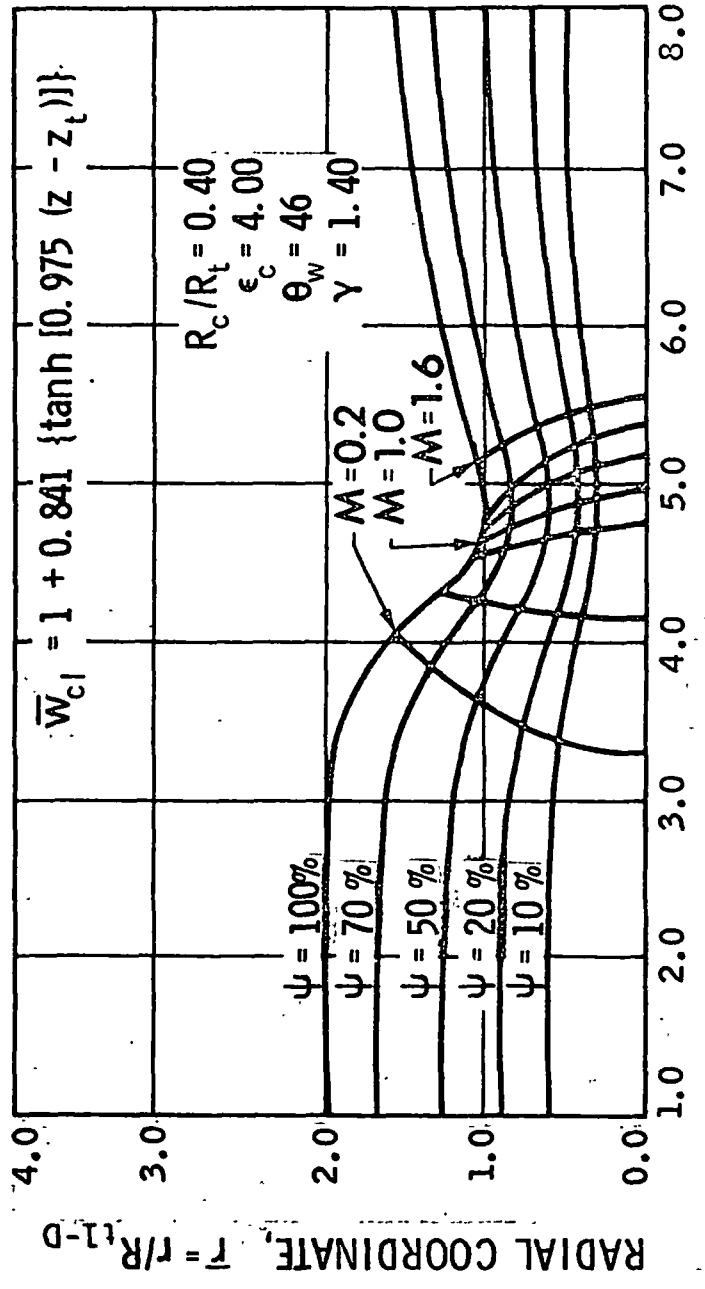

FIGURE 3. STREAMLINE DISTRIBUTION FOR $\gamma = 1.4$, $\epsilon_c = 4.0$

throats, and it causes the lines of constant Mach number to converge to a point near the minimum radius of the nozzle. Also the axial location for the minimum radius of a streamline tends to move upstream, while the nozzle inlet angle becomes more severe as the stream function increases.

Figure 4 presents the wall (Ψ = 100%) and centerline (Ψ = 0) pressures and Mach numbers as a function of axial position. The wall pressure exhibits two interesting details for this case. First, there is a relative maximum near the juncture of the convergent and cylindrical portions of the nozzle. This region has been troublesome in the past in that the boundary layer often separates due to the adverse pressure gradient[20]. This adverse pressure gradient becomes more severe with increasing θ_w. The value of the static pressure becomes close to the stagnation pressure indicating a virtual stagnation of the forward flow in some cases. Second, after the throat, there occurs another relative maximum. This phenomenon has been noticed in connection with conical nozzles where the exit cone joins the throat curvature. In Figure 3, the contour generated is analytic, therefore, the pressure rise must be associated with the compression experienced when the gases leave the throat curvature and are partially stagnated as they leave the circular arc and are forced into a more parallel flow. The Mach curve reflects the pressure fluctuations, in addition, it points to the large difference between the centerline and the wall Mach numbers. The one-dimensional value of Mach number, based on the Ψ = 100% contour is presented as a reference. Note that this

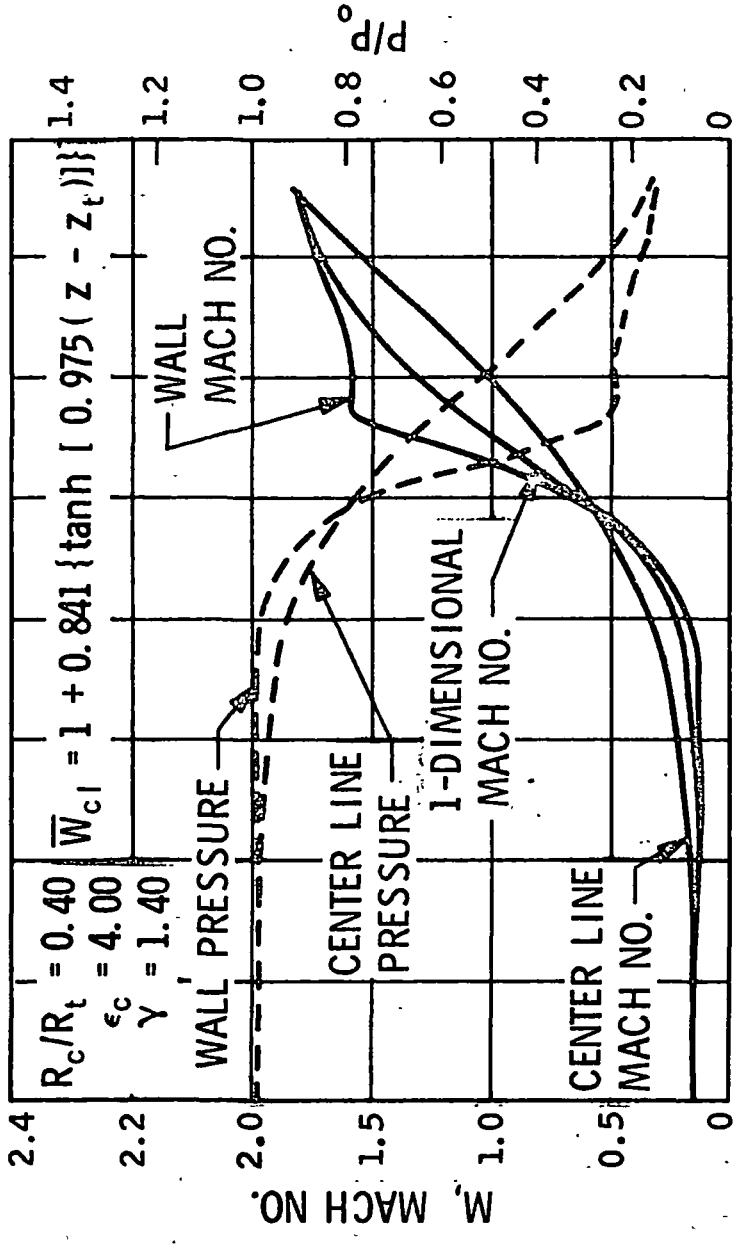

FIGURE 4. PROPERTY VARIATIONS WITH AXIAL LOCATION, $\gamma = 1.4$

value remains bounded by the wall and centerline value.

Figure 5 repeats the general pattern of Figure 3 except $\varepsilon_c = 9.0$. For this case,

$$A = 0.930$$

$$B = C = 0.760$$

$$z_t = 5.0$$

This centerline velocity function yields a nozzle in which,

$$R_c/R_t = 0.875, \text{ and } \theta_w = 50°.$$

For a given ε_c and R_c/R_t, the nozzle inlet, θ_w, may be tailored by varying the ratio of B/C in equation 27. To retain the same contraction ratio and radius of curvature ratio, A as well as (B + C) must be held constant. Figure 6 presents three cases illustrating the effect of varying B/C from 1.0 to 1.5 and 2.0. The coefficients for the velocity function are:

$$A = .931 \qquad \varepsilon_c = 9.0$$

$$B + C = 1.40 \qquad R_c/R_t = 1.15$$

$$z_t = 6.0$$

For Figure 5a the ratio B/C = 1.0 which results in a nozzle of $\theta_w = 55°$. When B/C = 1.50, the nozzle inlet angle reduced to $\theta_w = 42°$. When B/C = 2.0, the nozzle inlet angle was $\theta_w = 32°$. Thus, once a particular nozzle is identified for ε_c and R_c/R_t the inlet angle can be varied as desired by varying B/C.

After many runs were made, it was possible to arrive at a

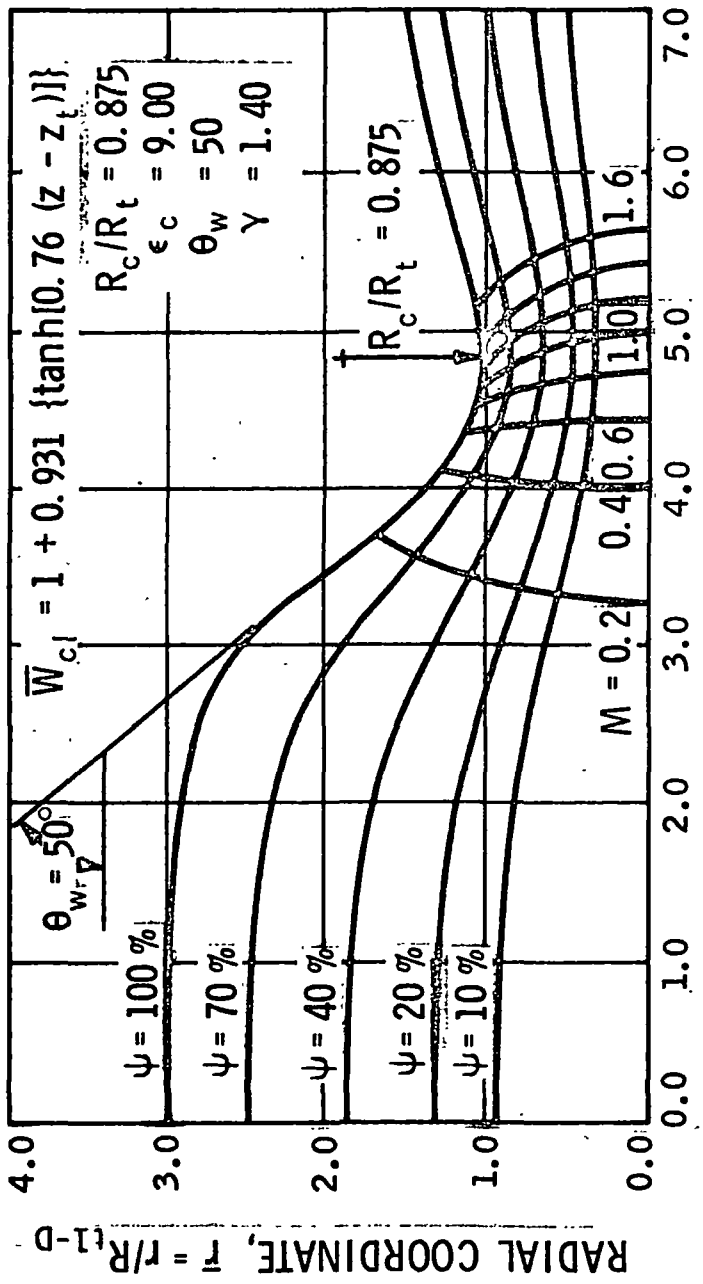

FIGURE 5. STREAMLINE DISTRIBUTION FOR $\gamma = 1.40$, $\epsilon_c = 9.00$

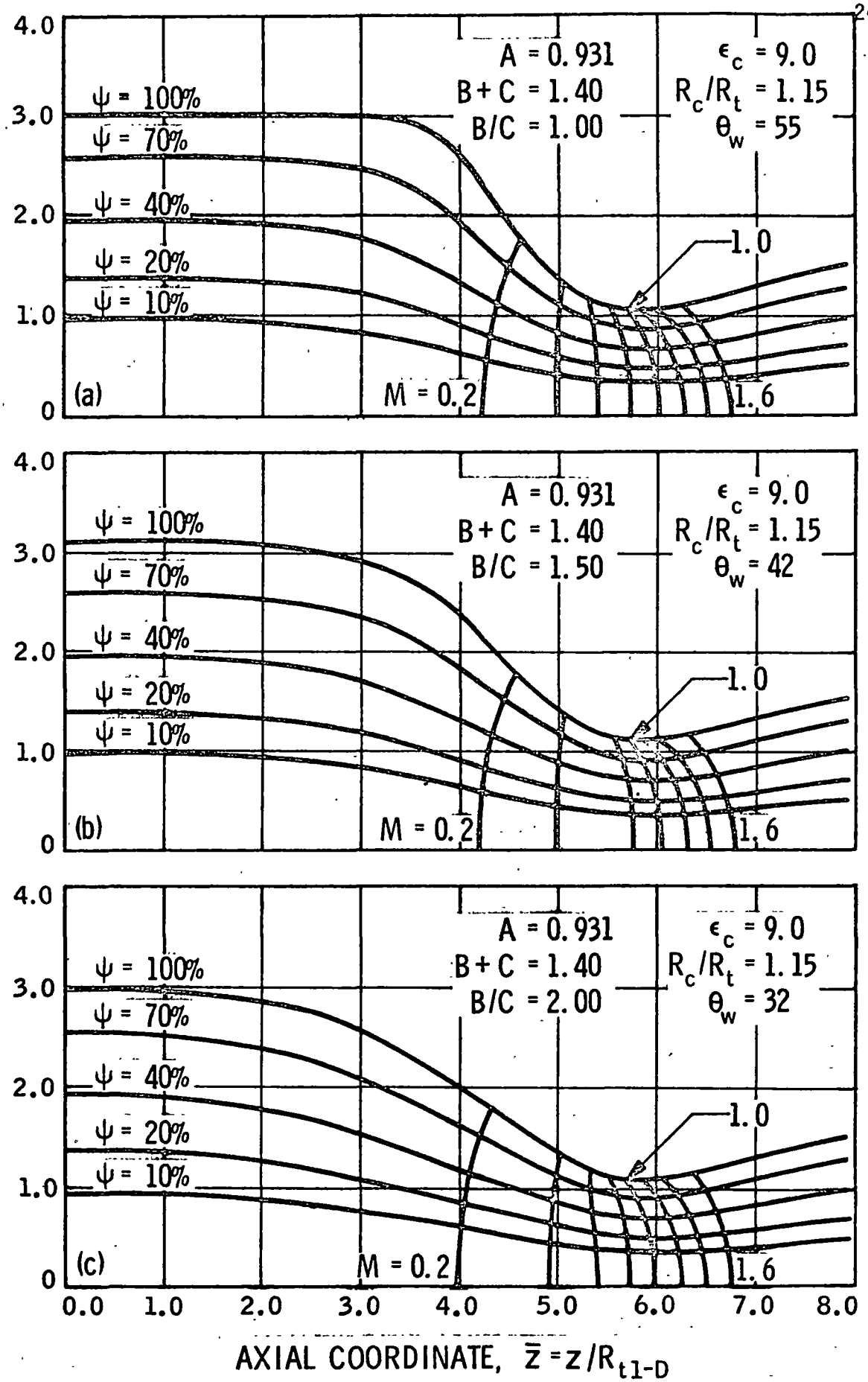

FIGURE 6. STREAMLINE DISTRIBUTION FOR $\epsilon_c = 9.0$, $\gamma = 1.40$, $R_c/R_t = 1.15$

generalized plot of R_c/R_t with respect to the coefficients of the centerline velocity function. Since there exists an infinity of nozzles corresponding to each particular velocity function depending on the streamline the results presented in Figure 7 reflect the value of the stream function as well. With this plot it is possible to choose the correct value of A(B + C) to yield the appropriate throat radius of curvature. It should be noted that this plot is approximate since the throat contours are only approximately circular.

Figure 8 presents the discharge coefficients with respect to R_c/R_t for some of the nozzles generated during the course of this study. It should be noted that the radius of curvature is not strictly defined for these studies, therefore, the best fit over an arc near the throat was used. The results of Kliegle and Levine's approximate theory based on a expansion about $1/(1 + R_c/R_t)$ are presented for reference[5].

The value of C_D was calculated for the present case by determining the minimum wall radius (streamline radius). In general, the two-dimensional solution yields a radius greater than the predicted one-dimensional value for the same mass flow. Therefore,

$$C_D = (R_{t\ 1\text{-}D}/R_{t\ 2\text{-}D})^2 \qquad (35)$$

The resultant C_D as a function of R_c/R_t was found to be essentially independent of θ_W. To prove this point several runs were made in which R_c/R_t was held constant however θ_W was varied from 55° to 32° (Figure 6). Within the accuracy of assigning a

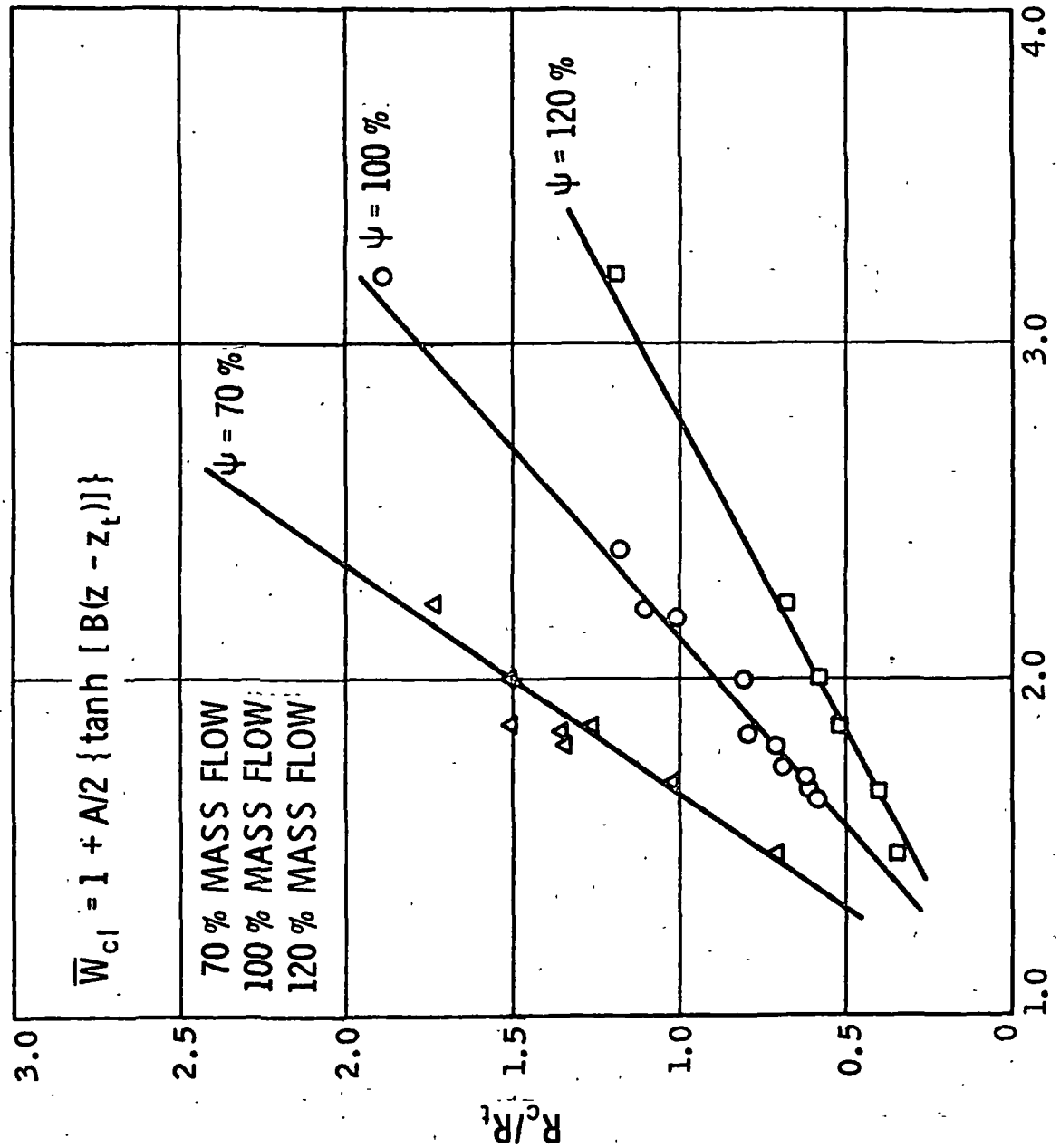

FIGURE 7. GENERALIZED RESULTS FOR R_c/R_t for $\gamma = 1.40$

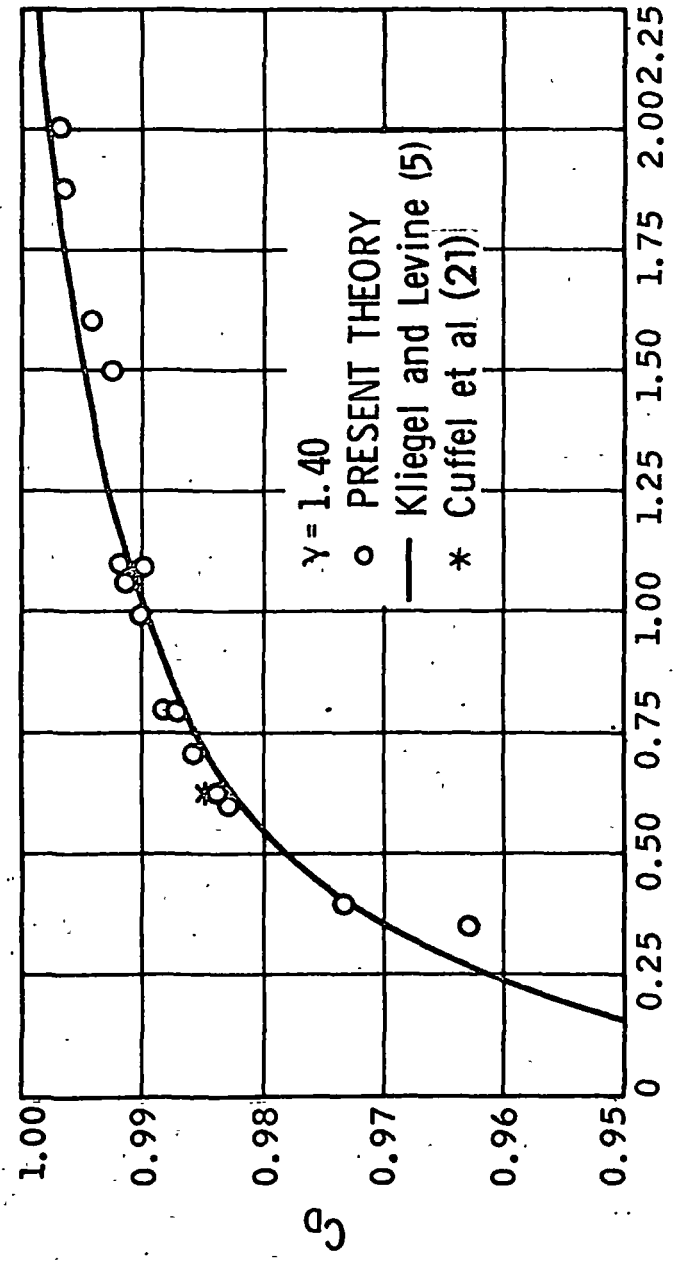

FIGURE 8. DISCHARGE COEFFICIENT WITH R_c/R_t

valve to R_c/R_t to the throat streamline contour, no variation in C_D was detected. Recently Back et al have gathered experimental data over a range R_c/R_t and θ_w. They concluded that except for R_c/R_t in the order of 0.25 and less, the θ_w dependence to be very small[19].

Figures 9 and 10 present the results of a nozzle generated for $\gamma = 1.20$. This specific heat ratio is more similar to rocket flows. The results are for a case where,

	$\gamma = 1.20$	$\gamma = 1.40$
$A = 0.843$	$R_c/R_t = 0.54$	$R_c/R_t = 0.40$
$B = 0.975$	$\varepsilon_c = 4.0$	$\varepsilon_c = 4.0$
$z_t = 5.00$	$\theta_w = 47^o$	$\theta_w = 46^o$

Thus, it is seen that reducing γ tends to decrease the R_c/R_t while retaining the same values of θ_w and ε_c.

Figures 11 and 12 present a nozzle which is compariable to one employed by Cuffel et al[21]. In this case some attempt was made to match the experimental nozzle wall, within the limit imposed by equation 27. Figure 11 illustrates the match obtained employing the standard centerline velocity function containing three arbitrary coefficients. From the transonic region upstream the match is very close. Also plotted are a few of the resultant lines of constant Mach number compared to experimental values. It can be seen that the experimental result show slightly greater curvature of the constant Mach lines. Figure 12 presents the centerline and wall Mach number in the region of the throat. The experimental results, again, show a more drastic variation at the throat.

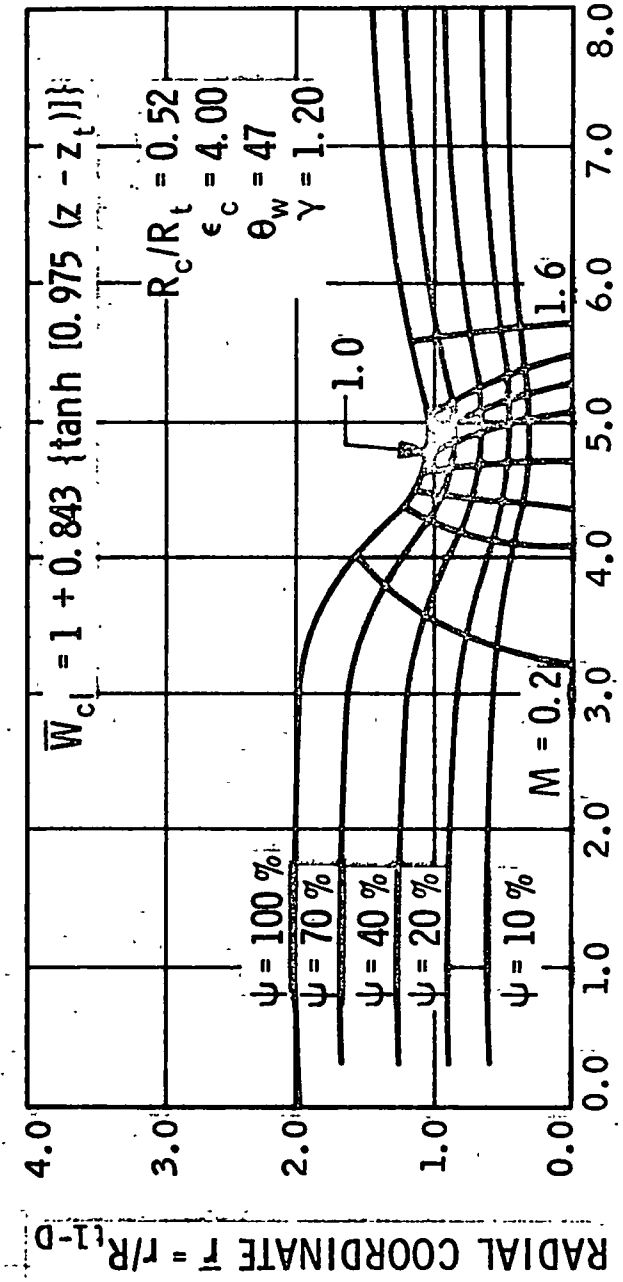

FIGURE 9. STREAMLINE DISTRIBUTION FOR $\gamma = 1.20$, $\epsilon_c = 4.0$

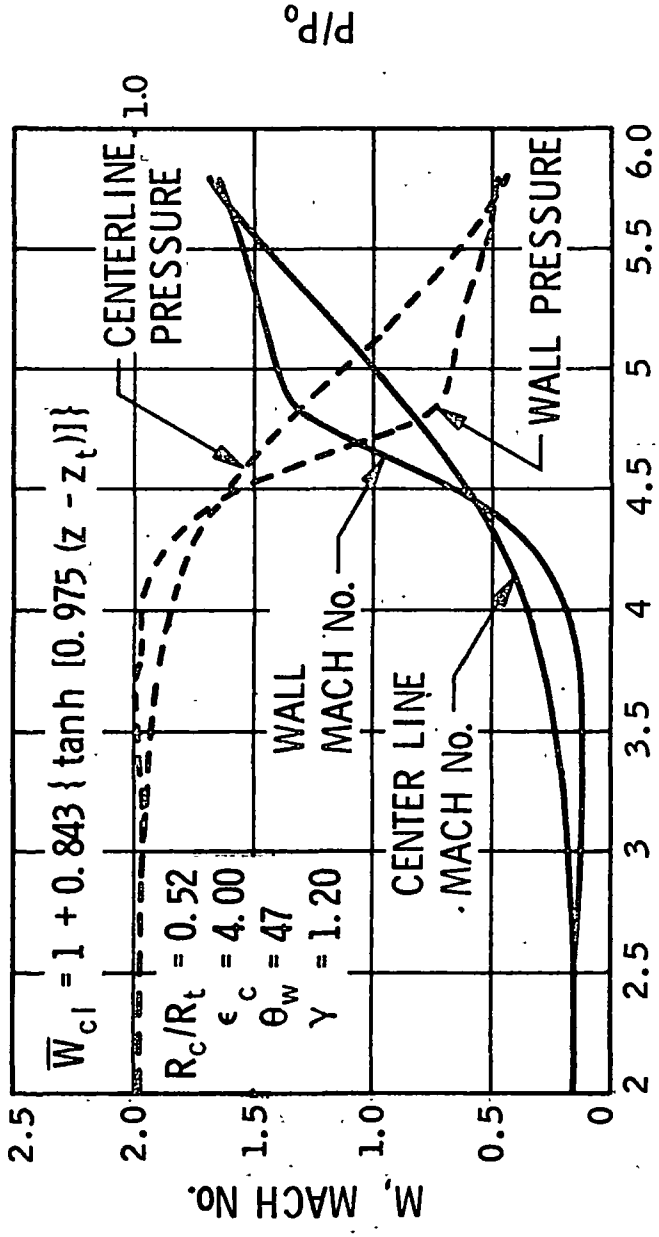

FIGURE 10. PROPERTY VARIATIONS WITH AXIAL LOCATION

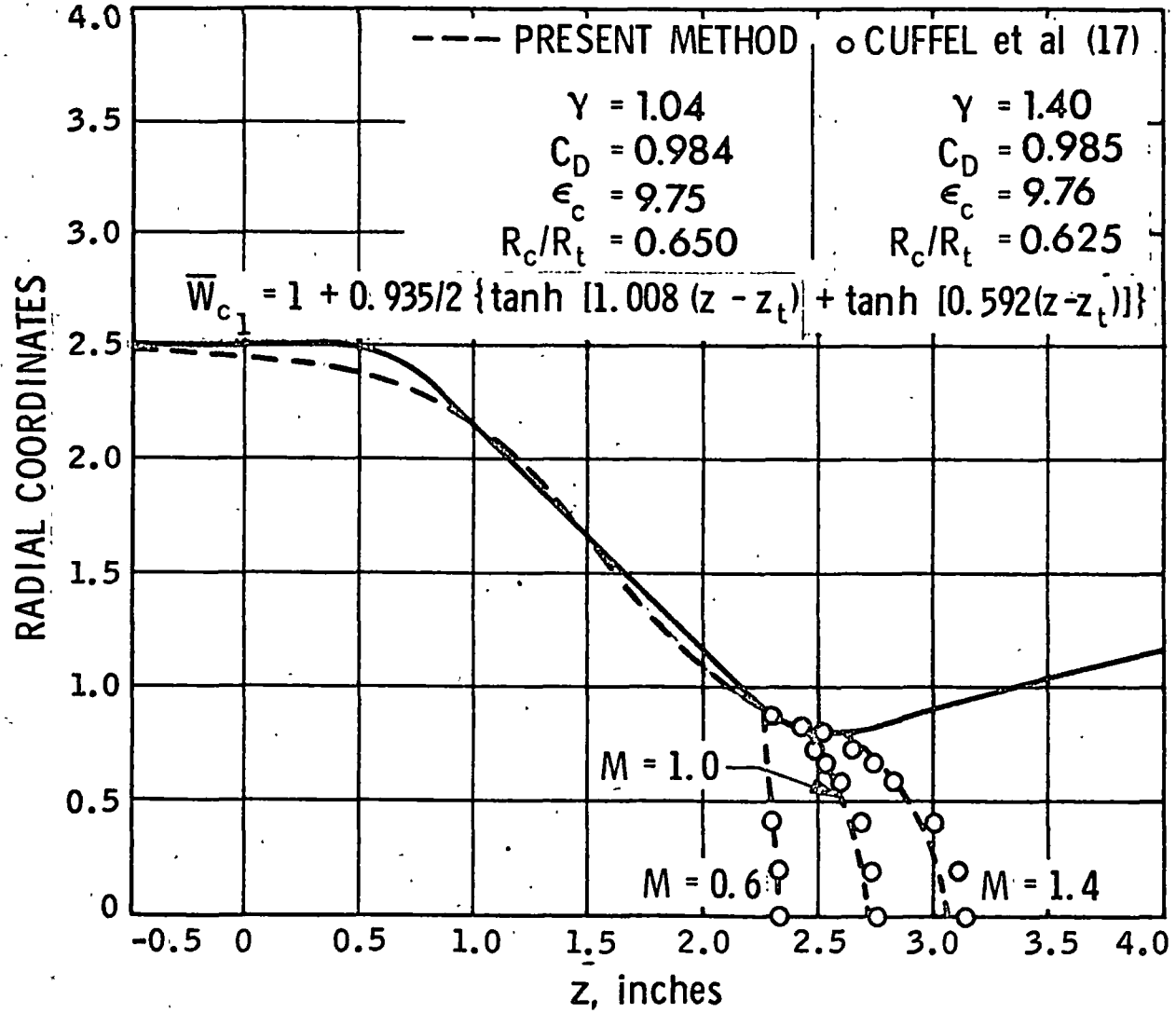

FIGURE 11. COMPARISON OF ANALYTICAL RESULTS WITH PUBLISHED DATA (21)

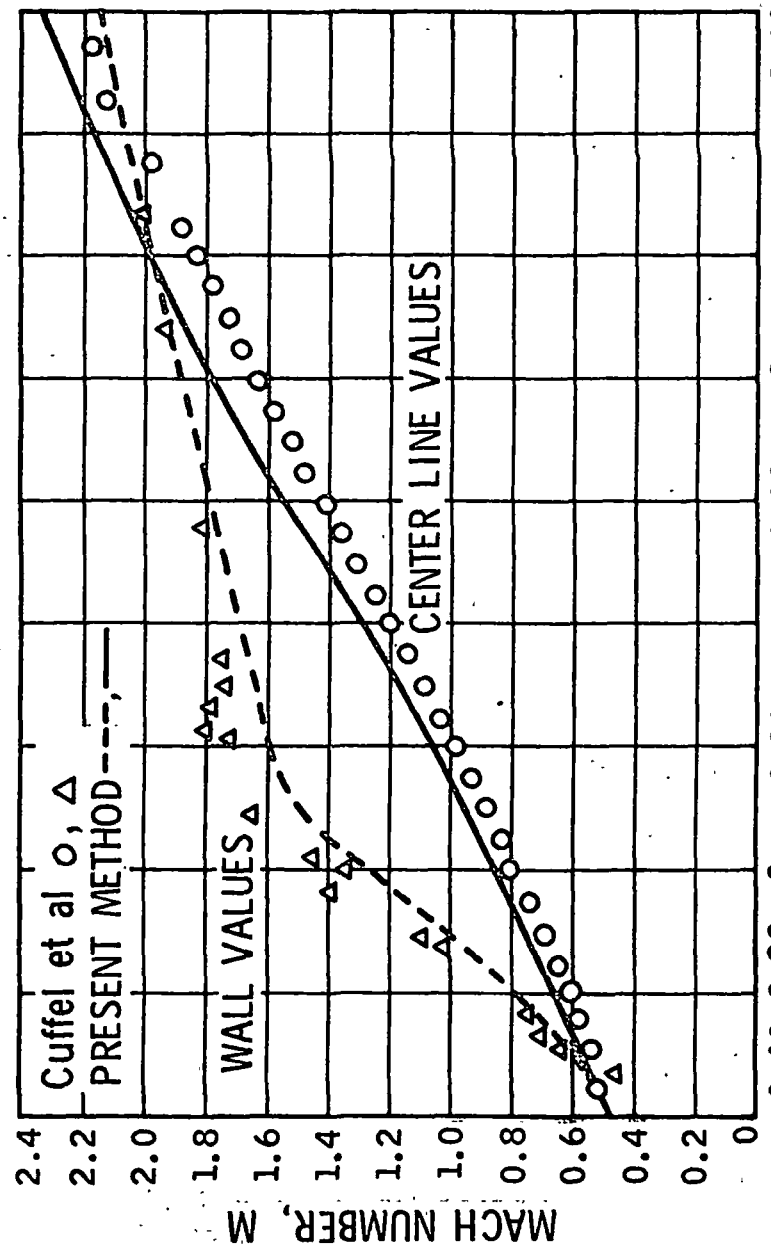

FIGURE 12. CENTERLINE AND WALL MACH NUMBERS COMPARED TO REFERENCE (17)

The differences between experimental and analytical results may be attributable to a number of factors. First, the contour generated is smooth and analytic throughout, while the experimental nozzle consists of straight lines and circular arcs. Second, there can be some round off or numerical smoothing found in any numerical difference method.

In this regard, no artificial or numerical viscosity was employed in there calculations, however the method is an implicit one which requires approximately three iterations per stream wise step. In view of the results compared to experimental ones a higher order difference scheme may be desirable especially when coupled with double precision operations. Third, there is the problem of accurate measurements in the transonic range. The quoted accuracy of the experiments was $\pm$ 0.2 psi based on a total pressure of 70 psi. In the throat region this causes the Mach number to be $\pm$ .02. It was interesting to note, however, that the discharge coefficient, C_D, for the experimental and analytical case agreed quite well. (See Figure 8).

STABILITY AND CONVERGENCE

During the course of this investigation there were many opportunities to test the convergence and stability of the present method. Some of the negative results obtained along the way to a successful technique should be of practical interest to other workers in the field. When the problem was first formulated, no axial stretching was attempted. Although some results were obtained, it was impossible to progress far into the Ψ direction before serious stabilities due to the lack of local convergence developed, even though an implicit method was employed.

The instability was nucleated at the point where the cylindrical section began to blend into the convergence portion of the nozzle. Characteristically, the velocity in the region is decreasing due to a locally adverse pressure gradient. This instability quickly spread upstream towards the initial conditions. Downstream of this point, no computing difficulties were encountered and smooth nozzle profiles were always obtained at the throat.

To circumvent these problems, the method of Lax-Wendroff[22] was employed. Now the essential function of the Lax-Wendroff method is to introduce an artificial, numerical viscosity (or diffusion coefficient, or heat transfer coefficient). In so doing, the form of the governing equations are changed from elliptic to hyperbolic. Naturally, the stability of the new hyperbolic problem initiated from cauchy conditions has been

found to be stable. Consider the following equation:

$$W_\psi + f_x = 0 \tag{36}$$

The finite difference analog for central differences is,

$$\Delta\psi^{-1} (W_{i,j+1}-W_{i,j})$$

$$+ (2\Delta x)^{-1} (f_{i+1,j}-f_{i-1,j}) \tag{37}$$

Employing the Lax-Wendroff method, the finite difference equation is written:

$$\Delta\psi^{-1}(W_{i,j+1}- 1/2 (W_{i-1,j} + W_{i+1,j}))$$

$$+ (2\Delta x)^{-1} (f_{i+1,j}-f_{i-1,j}) = 0 \tag{38}$$

Recasting the above expression yields,

$$\Delta\psi^{-1}(W_{i,j+1}-W_{i,j}) + (2\Delta x)^{-1}(f_{i+1,j}-f_{i-1,j})$$

$$= (2\Delta\psi)^{-1}(W_{i+1,j}$$

$$-2W_{i,j} + W_{i-1,j}) \tag{39}$$

Therefore, a subtle change in the form of the difference equations produces a drastic change in the equation to be solved

$$W_\psi + f_x = DW_{xx} \tag{40}$$

where,

$$D = \Delta x^2/2\Delta\psi \tag{41}$$

The magnitude of the artificial viscosity introduced is a strong function of the step sizes taken. Figure 12 presents the result of one calculation using this approach which led to a vastly improved stability. Further, the results were smooth and depended continuously on the initial conditions. Unfortunately the results were grossly in error, showing a spreading of Mach lines from the centerline to the wall, instead of converging at the throat.

At this point in the study, coordinate stretching was initiated. It was desired to place a large number of points in the transonic region while reducing the number of points in the low subsonic region. This permitted taking derivatives over physically large spaces where the velocity was not changing rapidly, while taking derivatives over small regions in the transonic region. Recall the stretching function given previously

$$\xi = 1 + \tanh\,(a(z-z_t)) \qquad (32)$$

This stretching function works well for nozzle flow patterns, however, others may be employed for different centerline velocity functions. Increasing the coefficient, a, results in grouping points at $z = z_t$. It is possible to take equal increments of ξ from 0. to 2.0 while providing optimum spacing of points in the physical plane. This technique permitted the removal of all artificial methods of convergence. Further it was possible to proceed well past the ψ = 100% condition. Two limits to the stability were noted. First, the coefficient a should be choosen in relation to the centerline velocity function. In other words, the more severe

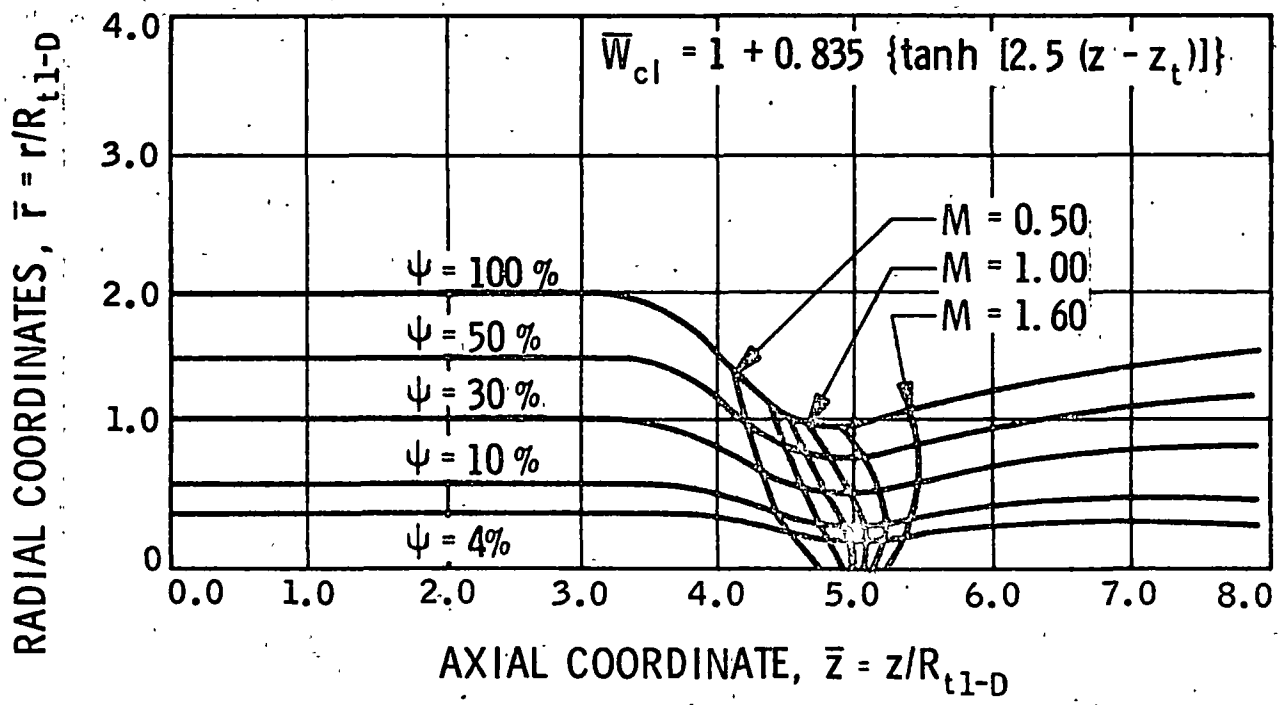

FIGURE 13. NOZZLE STREAMLINE DISTRIBUTION EMPLOYING THE LAX-WENDROFF METHOD

the gradients in W_{cl} the greater $\underline{a}$ should be. Second, when the nozzle inlet angle goes beyond 65^{o}, it is difficult to obtain convergence because the axial velocity is no longer the dominant variable in determining the mass flow rate. This means that the centerline axial velocity bears little influence on the results in this region.

CONCLUSIONS

The inverse method provides a powerful tool for the design of nozzles by calculating the flow field by one uniform approach from the surface of mass generation to the nozzle exit. The technique is not new, and has been applied to a variety of problems. In fact all of the approximate solutions for the transonic range apply this concept.[2-8] For inviscid flow no approximation in the governing equations need be made even for rotational flows. Therefore, within the accuracy of the numerical technique the solution is exact. Unfortunately, it is not possible to match a given nozzle wall contour completely with any finite term centerline velocity profile. However, since the shape of the subsonic portion is somewhat arbitrarily specified at the present time, this need be no real fault. A relatively simple centerline velocity function has been shown adequate to obtain any reasonable combination of ε_c, θ_w, R_c/R_t.

Solutions obtainable by this technique can be employed to yield a free stream condition for studies of such effects as separation, transition, and laminarization. In addition, interesting two-dimensional geometrical effects such as the influence of θ_w, R_c/R_t, and ε_c on C_D and the $M = 1$ condition can be investigated.

The success of the present method is largely due to the use of appropriate stretching functions for the axial coordinate so

that the grid spacing can be adjusted for optimum spacing. As one would suspect the lowest subsonic region causes the most difficulties. This is because in the finite difference sense, to advance in ψ requires more points of the centerline velocity to adequately describe the subsonic point. Coarse grid spacing in this region assures that the influence of $\bar{W}_{c_L}(z)$ over a large section is brought to bear on the low Mach number points. Concentrating the grid in the transonic region permits only relatively local effects to dominate and allows greater accuracy where velocity gradients are highest.

A final word concerning the inverse technique applied to mixed flows (subsonic, transonic and supersonic) seems appropriate. It may be of some concern that the centerline velocity function is specified every where apriori. This means that the supersonic flow can indeed influence the subsonic flow. If this is troublesome, recall that the streamline contour is not fixed apriori but is calculated iteratively. In other words, it is not surprising that a movement of the streamline contour should effect both the subsonic and supersonic flow.

NOMENCLATURE

A, B, C = constants in centerline velocity function

C_D = nozzle discharge coefficient

c_p = specific heat at constant pressure

f = orbitrary function

H = enthalpy

M = Mach number

P = pressure

$\bar{q}$ = velocity vector

r, θ, z = cylindrical coordinates

R = gas constant

R_c = throat radius of curvature

R_t = throat radius

S = entropy

T = temperature

u, v, w = radial, tangential, and axial velocities

γ = specific heat ratio

Δ = finite difference

ε = contraction or expansion ratio

ξ = transformed axial coordinate

θ_w = nozzle wall inlet angle

ν = iteration number

π = 3.14159...

ρ = density

ψ = stream function

Subscripts

c = throat curvature radius, contraction

cl = centerline

inf = infinity

o = stagnation conditions

t = throat valve

1-D = one dimensional

i = axial grid point designation

n = streamline grid point designation

Superscripts

- nondimensional value

' derivative with respect to z

REFERENCES

1. Guderly, K. G., The Theory of Transonic Flow, Addison-Wesley Publishing Company, Inc., Reading, Mass., 1962, p. 68.

2. Oswatitsck, K. and Rothstein, W., "Flow Pattern in a Converging-Diverging Nozzle," NACA Lewis Research Center, TM 1215, 1949.

3. Sauer, R., "General Characteristics of the Flow Through Nozzles at Near Critical Speeds," NACA Lewis Research Center, TM 1147, 1947.

4. Hall, I. M., "Transonic Flow in Two-Dimensional and Axially-Symmetric Nozzles," Quarterly Journal of Mechanics and Applied Mathematics XV, 487-508, 1962.

5. Kliegel, J. D., and Levine, J. N., "Transonic Flow in Small Throat Radius of Curvature Nozzles," AIAA Journal, Vol. 7, No. 7, July 1969, pp. 1375-1378.

6. Levine, J. N., Coar, D. E., "Transonic Flow in a Converging-Diverging Nozzle," NASA-CR-111104, Sept. 1970.

7. Hopkins, D. F. and Hill, D. E., "Effect of Small Radius of Curvature on Transonic Flow in Axisymmetric Nozzles," AIAA Journal 4, 8, 1337-1343, (Aug. 1966).

8. Friedricks, K. O., "Theoretical Studies on the Flow Through Nozzles and Related Problems," Applied Mathematics Group, New York University, Report 82.1R, AMG-NYU 43 (1944).

9. Morris, P. M. and Feshback, H., Methods of Theoretical Physics, McGraw-Hill Book Company, New York, 1953, Vol. 1, p. 706.

10. Crocco, L., "A Suggestion for the Numerical Solution of the Steady Navier-Stokes Equations," AIAA Journal, Vol. 3, No. 10, Oct. 1965, pp. 1824-1832.

11. Migdal, D., Klein, K., and Moretti, G., "Time-Dependent Calculations for Transonic Nozzle Flow," AIAA Journal, 7, 2, pp. 372-373, Feb. 1969.

12. Prozan, R. J., Work referred to in reference 21.

13. Pirumov, U. G., "Calculation of the Flow in a Laval Nozzle," Soviet Physics-Doklady, Vol. 12, No. 9, pp. 857-860, March 1968.

14. Courant, R. and Hilbert, D., Methods of Mathematical Physics, Vol. II, Interscience Publishers, New York, 1962.

15. Hardamard, J., Lectures on Cauchy's Problem in Partial Differential Equations, Dover Publications, New York, 1952.

16. Back, L. H., Massier, P. F., and Cuffel, R. F., "Some Observations on Reduction of Turbulent Boundary-Layer Heat Transfer in Nozzles. AIAA Journal, Vol. 4, No. 12, Dec. 1966, pp. 2226-2229.

17. Back, L. H., Massier, P. F., Cuffel, R. F., "Flow and Heat Transfer Measurements in a Subsonic Air Flow Through a Contraction Section," International Journal of Heat and Mass Transfer, Vol. 12, Jan. 1969, pp. 1-13.

18. Frank, L. S., "Difference Methods for Solving the Improper Cauchy Problem Simulating Flow of a Perfect Gas Through a Nozzle," Soviet Physics-Doklady, Vol. 13, No. 9, March 1969.

19. Back, L. H., Cuffel, R. F., "Flow Coefficients for Supersonic Nozzles with Comparatively Small Radius of Curvature Throat," AIAA Journal, Vol. 8, No. 2, Feb. 1970, pp. 196-198.

20. Back, L. H., Massier, P. F., and Cuffel, R. F., "Effect of Inlet Boundary-Layer Thickness and Structure on Heat Transfer in a Supersonic Nozzle," AIAA Journal, Vol. 5, No. 1, pp. 121-123, Jan. 1968.

21. Cuffel, R. F., Back, L. H., and Massier, P. F., "Transonic Flowfield in a Supersonic Nozzle with Small Throat Radius of Curvature," AIAA Journal, Vol. 7, No. 7, pp. 1364-1366, July 1969.

22. Lax, P. D., and Wendroff, "Difference Schemes of Hyperbolic Equations with High Order Accuracy," Comm. Pure and Applied Math, Vol. 17, 1964, pp. 381-398.